# Optimization of Brain T₂ Mapping using Standard CPMG Sequence in a Clinical Scanner

P. Hnilicová, M. Bittšanský, D. Dobrota

Department of Medical Biochemistry, Jessenius Faculty of Medicine, Comenius University, Mala hora 4, 036 01 Martin, Slovakia, petra.hnilicova@jfmed.uniba.sk

In magnetic resonance imaging, transverse relaxation time ($T_2$) mapping is a useful quantitative tool enabling enhanced diagnostics of many brain pathologies. The aim of our study was to test the influence of different sequence parameters on calculated $T_2$ values, including multi-slice measurements, slice position, interslice gap, echo spacing, and pulse duration.

Measurements were performed using standard multi-slice multi-echo CPMG imaging sequence on a 1.5 Tesla routine whole body MR scanner. We used multiple phantoms with different agarose concentrations (0 % to 4 %) and verified the results on a healthy volunteer.

It appeared that neither the pulse duration, the size of interslice gap nor the slice shift had any impact on the $T_2$. The measurement accuracy was increased with shorter echo spacing. Standard multi-slice multi-echo CPMG protocol with the shortest echo spacing, also the smallest available interslice gap (100 % of slice thickness) and shorter pulse duration was found to be optimal and reliable for calculating $T_2$ maps in the human brain.

Keywords: Magnetic resonance imaging, relaxation time, $T_2$ mapping, brain, phantom.

## 1. INTRODUCTION

IN RECENT YEARS magnetic resonance imaging (MRI) has become an important medical imaging method [1], [2]. $T_2$ weighted MRI scans are used for the analysis of the diseased brain tissue. The method is based on the fact that pathologic and normal tissues have different $T_2$ relaxation times [3] – [7]. $T_2$ images are known as "pathology scans" [8], [9]. It has been shown that measurement of the change in $T_2$ provides important information about the mobility and chemical environment of the tissues of interest [4], [9] – [11]. Previous studies examining the utility of $T_2$ mapping in the context of neurologic and psychiatric disease demonstrated variations in $T_2$ values, sometimes very subtle, in specific brain regions within conditions of autism [12], schizophrenia [13], [14], epilepsy [15], Parkinson's [16], multiple sclerosis [17], [18], Alzheimer disease [9], tumors [19], [20], [21] and a host of other disorders [6], [14], [16], [22], [23]. Nevertheless, mapping the $T_2$ parameter is rarely used in clinical diagnostics, the most common reported reasons being higher scanning times [4], [6], [10], [11] or its lack of specificity, in contrast to its high sensitivity [5], [6], [17], [24]. In clinical studies, $T_2$ relaxation data is most commonly obtained from single-slice MR sequences [15], [24] – [27]. For tissue mapping purposes, a multi-slice sequence is more suitable.

In clinical scanners, the number of adjustable sequence parameters and their ranges are quite limited. In order to exploit the advantages of $T_2$ mapping in clinical environment, we decided to experimentally verify the reliability of a standard Carr-Purcell Meiboom-Gill (CPMG) [28] multi-slice multi-echo sequence for $T_2$ mapping. To our knowledge, it is the most widely used sequence for $T_2$ mapping [3], [9] – [11], [24] – [27], [29] – [32]. In addition, a multi-echo approach enables rapid $T_2$ mapping of tissues and is therefore optimal for the use in patient measurements. The aim of our study was to analyze the influence of different measurement parameters such as the number of slices, slice position, interslice gap, echo spacing, and pulse duration on the measured $T_2$ relaxation times in a routine clinical scanner. This study included preparation of a suitable phantom, multiple $T_2$ measurements with different sequence parameters, and data analysis on a custom-made software, in order to obtain useful information of $T_2$ mapping for future clinical studies. Therefore, we verified the results of our study by calculating the $T_2$ maps of a human brain in a healthy volunteer.

## 2. MATERIALS & METHODS

### 2.1. Phantom and volunteer for $T_2$ mapping.

For the phantom preparation, we chose agarose, a plant-based jellifying agent commonly used for MRI phantom measurements. This is because of its mechanical and imaging characteristics similar to those of soft tissues [33], [34]. With phantom measurements for a reliable $T_2$ mapping, it is necessary to cover the range of $T_2$ relaxation times of the human brain (40 – 150 ms) [3], [24] – [26]. In this study we used 5 pairs of phantoms with agarose concentrations of 0 %, 1 %, 2 %, 3 % and 4 %. A weighted amount of the agarose powder (A9539, SIGMA-ALDRICH, SK) was mixed with distilled water to make up a total volume of 20 ml for each agarose concentration. The mixture was heated over 85°C to completely dissolve the agarose. It was then poured into colorless plastic tubes and cooled until gelatinous. Finally, the tubes were sealed with a lid to prevent any water loss [33] – [35]. All phantoms were placed in a plastic holder and immersed in a water bath of approximately 1.5 liters to avoid abrupt susceptibility changes in the edges of the phantoms.

Based on the results of the phantom measurement, in the second phase of our study, $T_2$ mapping of the brain was verified on a volunteer, a 23 years old male without previous brain injury or surgery, or a history of neurological disease, psychiatric illness or substance abuse.

## 2.2. MRI examination.

The MR measurements were performed on a clinical 1.5 Tesla whole-body MR scanner Magnetom Symphony (Siemens, Erlangen, Germany) using the standard ^{1}H quadrature volume head-coil. Measurements were made at an ambient temperature of 23°C.

Standard Carr-Purcell Meiboom-Gill (CPMG) multi-spin-echo imaging sequence was used, which consisted of a 90° RF pulse followed by an echo train induced by successive 180° pulses (90°→180°-echo1→180°-echo2 …). Between the 90° pulse and the subsequent 180° pulses was a phase shift in the rotating frame of reference in order to reduce accumulating effects of imperfections in the 180° pulses [36]. For $T_2$ relaxation measurement we used the following parameters: in-plane resolution of 3.3x2.2 mm$^2$, a slice thickness of 4 mm, a field of view of 157 x 280 mm$^2$, one average, a base resolution of 72 x 128 pixels; number of slices: 1 for single-slice and 19 for multi-slice; TR = 8860 ms. The multi-slice sequence included a series of 32 different TEs with 3 different types of (equal) echo spacing listed below:

a) echo spacing of 7 ms: TEs [ms] = 7, 14, 21, … 224

b) echo spacing of 10 ms: TEs [ms] = 10, 20, 30, … 320

c) echo spacing of 20 ms: TEs [ms] = 20, 40, 60, … 640.

The *Syngo* user interface offers two types of sinc-shaped RF pulses for $T_2$ mapping sequences, "NORMAL" pulse with shorter duration (2.56 ms) and "lowSAR" pulse with longer duration (3.84 ms), for both 90° and 180° pulses (Fig.1.) [37], [38]. All our measurements of the $T_2$ relaxations were performed with the application of both pulse durations. The total acquisition time for various CPMG settings was 6 minutes and 21 seconds.
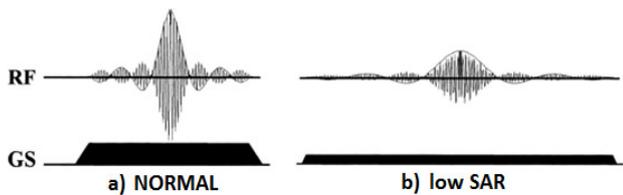


Fig.1. a, b. "NORMAL" and "low SAR" pulses.
The course of a "NORMAL" and "low SAR" RF pulse used in $T_2$ mapping sequences. GS means slice selection gradient [37].

In our study, we measured an echo spacing of 10 ms and 20 ms with a bandwidth of 275 Hz per pixel, and an echo spacing of 7 ms with a bandwidth of 501 Hz per pixel (the lower bandwidth was not achievable at 7 ms echo spacing due to the sequence timing).

In order to see the impact of the position of slices within the tissue on the $T_2$ mapping; we first measured one particular section of the phantom (and brain tissue) using a single-slice. Then we measured the same slice using a multi-slice sequence, with the given slice in the center (10th of 19 slices) or close to the boundary (2nd of 19 slices) of the slice package. In addition, we also compared the data for these slices with those of their neighboring slices.

To assess any influence of the distance between the slices on the measured $T_2$ values we performed measurements using a 100 % and a 130 % inter-slice gap with 100 % being the minimum available for this sequence set by the manufacturer (100 % meaning the same empty gap between the slices as the slice thickness itself).

In order to quantify the $T_1$ relaxation of the phantom and the volunteer, we performed MR imaging with the following parameters: spin-echo progressive-saturation sequence, nominal resolution of 74 x 192, a slice thickness of 8 mm (6 mm in the volunteer), a field of view of 175 x 300 mm$^2$, one average; nine different repetition times (TR) [ms] = 25, 50, 100, 200, 400, 700, 1000, 3000, 10000; a constant echo time (TE) of 5 ms.

All the measurements were performed within one session, in the phantoms as well as on the volunteer.

## 2.3. Data evaluation.

Data was processed using a home-written code in Matlab (Math Works, Natick, MA). The program was able to iteratively fit $T_1$ and $T_2$ relaxation curves using the Levenberg-Marquardt algorithm on a pixel-by-pixel basis and to display fitted parameters for every selected pixel, including relaxation times ($T_2$ or $T_1$), and the initial magnetization ($M_0$). The fitting algorithm was based on the mathematical functions for $T_1$ calculation (1), where $T_1$ is the relaxation time, for which the amplitude of the magnetization vector ($M_z$) reaches approximately 63 % of the fully-relaxed magnetization ($M_0$) [39], [40].

$$M_z = M_0 \left( 1 - e^{-\frac{TR}{T_1}} \right) \quad (1)$$

For $T_2$ relaxation (Fig.2.), we used the (2), where $T_2$ is the relaxation time for which the amplitude of the magnetization vector ($M_{xy}$) decreases to approximately 37 % of the maximum magnitude $M_0$ [4], [39].

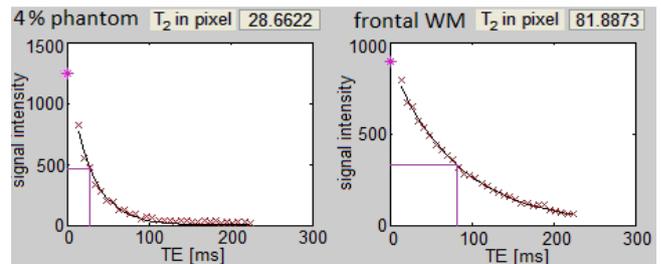$$M_{xy} = M_0 \left( e^{-\frac{TE}{T_2}} \right) + N \quad (2)$$



Fig.2. $T_2$ relaxation fit.
The $T_2$ relaxation fit; one pixel in 4 % phantom with short $T_2$ and one sample from frontal white matter (WM) in the healthy brain.

Noise ($N$) was estimated in the equation as an average signal intensity of 62 pixels (2 pixels from the 2 upper corners of each image across 31 images in the set), which excluded any signal coming from the measured object. Our program also generated maps of particular relaxation parameters and allowed for evaluation of regions of interest (ROIs), with identical ROIs positions for different images. The program evaluated parameters in the calculated maps on a pixel-by-pixel basis and displayed their mean values and standard deviations within the ROIs.

In addition to the multi-slice measurement, we compared the data from the selected slices to the data from their neighboring slices. Given the fact that the most of the artifacts are in the first echo of the multi-echo sequence, we decided to omit the first echo and evaluate only the remaining 31 echo series.

For each agarose phantom, we evaluated 3 pixels in the center of its cross-section, so we used the data of 6 voxels for each agarose concentration (Fig.3.a). For the $T_2$ (or $T_1$) mapping of the volunteer we evaluated 3 pixels bilaterally each time placed in 8 regions of the brain (frontal white matter; frontal gray matter; temporal gray matter; parietal gray matter; occipital gray matter; caudate nucleus; putamen and thalamus) as seen in Fig.3.b.
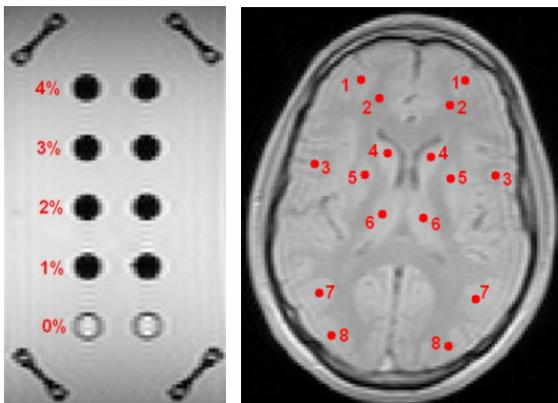


Fig.3. a, b. MR image of phantoms and the healthy human brain. The cross-section of the $T_2$-weighted MRI shows 5 pairs of phantoms with agarose concentrations 0 %, 1 %, 2 %, 3 % and 4 % placed in the holder.
$T_1$-weighted MRI on the right shows 8 evaluated regions bilaterally placed in the brain: 1) frontal gray matter; 2) frontal white matter; 3) temporal gray matter; 4) caudate nucleus; 5) putamen; 6) thalamus; 7) parietal gray matter; 8) occipital gray matter.

## 3. RESULTS

### 3.1. Results from phantom measurements.

First, we measured $T_1$ values of the phantoms. We observed that with increasing agarose concentration (0, 1, 2, 3 and 4 %), the value of $T_1$ significantly decreased (2812 ± 65, 2662 ± 41, 2470 ± 41, 2164 ± 50 and 1849 ± 65 ms, respectively; one-way ANOVA).

Then we studied the effect of $T_1$ relaxation, number of slices, pulse duration, echo spacing, bandwidth, interslice gap and slice shifting to the calculated values of $M_0$ in $T_2$ maps (Fig.4.). To be able to compare different measurements, we evaluated the average noise in pictures. The value of noise in the image did not change significantly (unpaired t test) with different pulse duration, number of slices, inter-slice space, slice shifting, echo spacing or bandwidth.

There was no significant difference (NS, one-way ANOVA) in $M_0$ values between various agarose concentrations, if the other parameters were kept constant. Significantly greater (**, one-way ANOVA) $M_0$ was found in the single-slice method in comparison with the multi-slice measurements. A significantly greater $M_0$ (**, unpaired t test) was achieved with "lowSAR" pulse duration than with "NORMAL" at the same echo spacing and bandwidth. Neither the size of the interslice gap nor the slice position in the multi-slice measurement significantly affected (unpaired t test) the values of $M_0$.

In our next step, we investigated the influence of measurement parameters on the calculated value of $T_2$ in phantoms (Fig.5.). Increasing agarose concentration (0, 1, 2, 3 and 4 %) led to a decrease of the $T_2$ relaxation time (for example, in single-slice with "NORMAL" pulse duration, echo spacing 7 ms, bandwidth 501 Hz per pixel: 2208 ± 29, 112 ± 5, 67 ± 5, 40 ± 5 and 28 ± 5 ms). There were significant differences (one-way ANOVA) in the obtained $T_2$ values among the phantoms with longer $T_2$ relaxation times (0 %, 1 %, 2 % and 3 %), whereas in the case of short $T_2$ relaxation times (3 vs. 4 %) there were no significant effects (one-way ANOVA). We observed the same behavior when using both types of pulse durations and in single- as well as in multi-slice measurements (with 100 % and 130 % interslice gaps). No significant differences (NS, unpaired t test) in $T_2$ values were observed with the "lowSAR" pulse duration compared to "NORMAL" at the same echo spacing and bandwidth. No significant differences (one way ANOVA) were also found when we compared the $T_2$ values of the phantoms calculated from a measurement using "NORMAL" pulses, 7 ms echo spacing and 501 Hz per pixel bandwidth with a measurement using "lowSAR" pulses, 10 ms echo spacing and 275 Hz per pixel bandwidth. Neither the size of interslice gap nor the slice shifting had any impact on the calculated $T_2$ relaxation times.

We analyzed the variance of standard deviation (SD) in the $T_2$ values obtained using 6 pixels from each agarose concentration (Fig.6.a, b). Larger variances in SD were observed for the shorter $T_2$ relaxation times. We found that SDs were not significantly different (one way ANOVA) between pulses "NORMAL" and "lowSAR". Then, we compared measurements with echo spacing 20 ms and 10 ms. It was confirmed that smaller echo spacing decreased the variances in SD in phantoms with shorter $T_2$s without a significant impact on the $T_2$ relaxation time.
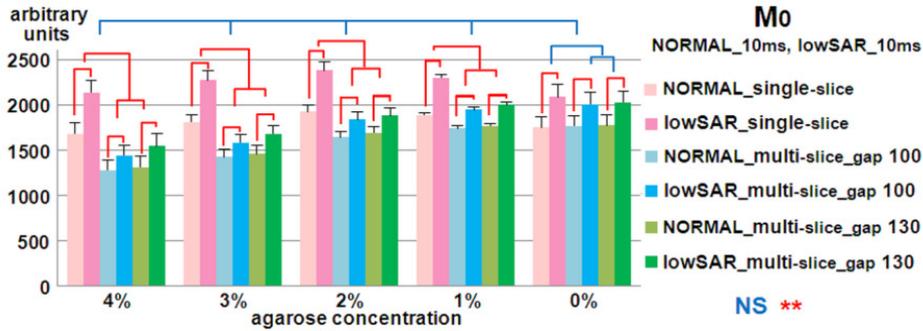
Fig.4. $M_0$ values in phantoms.
There were no significant differences (NS, one-way ANOVA) in $M_0$ values between 0, 1, 2, 3 and 4 % agarose concentrations. A significantly greater $M_0$ (**, one-way ANOVA) was found in single-slice measurement when compared to multi-slice. For the pulse duration "lowSAR", a significantly greater $M_0$ (**, unpaired t test) was found when compared to the pulse duration "NORMAL" at the same echo spacing (10 ms) and bandwidth (275 Hz per pixel). It appeared that the size of the interslice gap did not significantly affect the calculation of $M_0$.
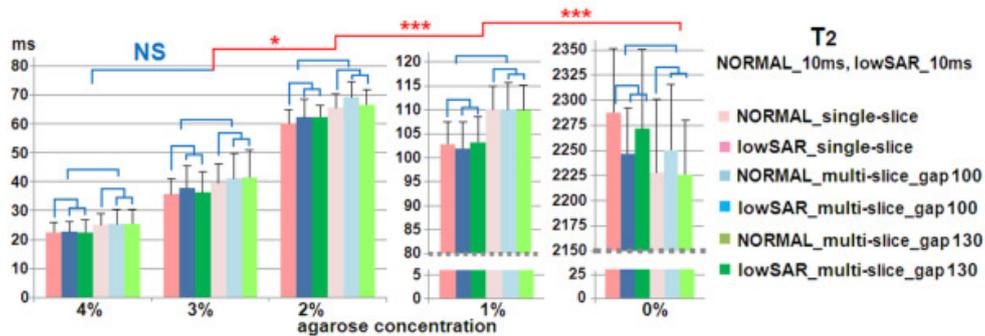


Fig.5. $T_2$ values in phantoms.
Decreasing agarose concentration (4 – 0 %) increased the $T_2$ values of phantoms. There were significant differences in $T_2$ values between the phantoms with longer $T_2$ relaxation: 3 % vs. 2 % (*); 2 % vs. 1 % (***); 1 % vs. 0 % (***) (one-way ANOVA). In phantoms with shorter $T_2$ relaxation, $T_2$ values were not significantly different: 3 % vs. 4 % (NS; one-way ANOVA). The pulse duration ("NORMAL" or "lowSAR") did not affect the $T_2$ relaxation time (NS; unpaired t test) at the same echo spacing (10 ms) and bandwidth (275 Hz per pixel). Non-significant differences in $T_2$ values were found between single-slice and multi-slice measurements (NS, one-way ANOVA). The size of the interslice gap has no impact on the $T_2$ relaxation times.
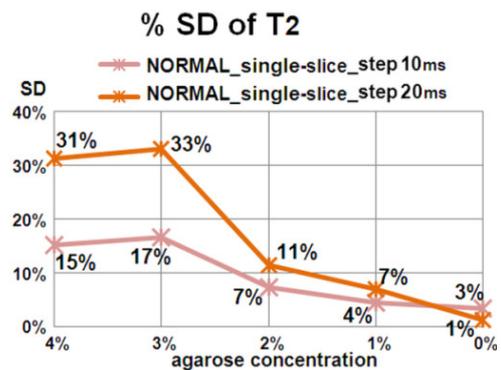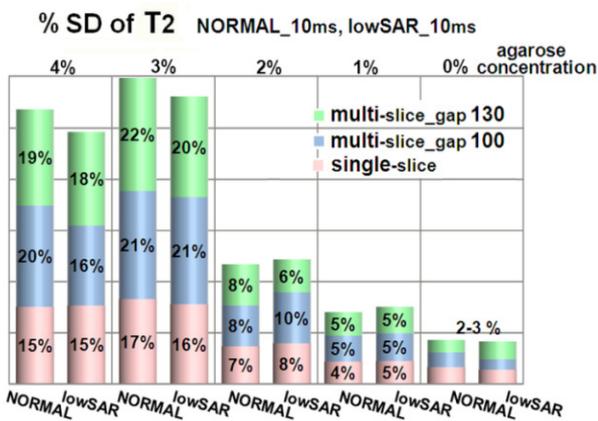


Fig.6. a, b. Standard deviation (SD) in phantom $T_2$ values.
The SDs of $T_2$ values were not significantly different (one way ANOVA) between the pulse duration of "NORMAL" and "lowSAR" or between single- and multi-slice. The size of the interslice gap had no impact on the SD variance of $T_2$ values. The largest variance in SD (~ 20 %) was observed in phantoms with a shorter $T_2$ relaxation (4 %, 3 %). In the case of phantoms with a longer $T_2$ relaxation (2 %, 1 %, 0 %), the SD was under 10%. The measurement with a shorter echo spacing (10 ms) had a lower SD of $T_2$ values in comparison to the longer echo spacing (20 ms) measurements.

### 3.2. Results from the measurement of the volunteer.

First, we measured the $T_1$ values of the volunteer's brain, which were: $699 \pm 19$ [ms] in the white matter, $1155 \pm 40$ [ms] in the frontal lobe, $1245 \pm 56$ [ms] in the temporal lobe, $1171 \pm 81$ [ms] in the parietal lobe, $1229 \pm 75$ [ms] in the occipital lobe, $964 \pm 27$ [ms] in the putamen, $992 \pm 28$ [ms] in the thalamus and $1188 \pm 37$ [ms] in the caudate nucleus.

We also measured the effect of the number of slices, pulse duration, echo spacing, bandwidth, interslice gap and slice shifting on the value of $M_0$ (Fig.7.). $M_0$ values in single-slice were significantly higher (**, one-way ANOVA) compared to $M_0$ values in multi-slice. The pulse duration of "NORMAL" or "lowSAR" did not affect the calculation of $M_0$ (NS, unpaired t test). Moreover, with "NORMAL" pulses and short echo spacing (7ms), the $M_0$ values were not significantly different from those in the "lowSAR" pulse, which had longer echo spacing and a smaller bandwidth. For the calculation of $M_0$, no significant effect of varying interslice gaps (NS, unpaired t test) or slice shifting was observed.
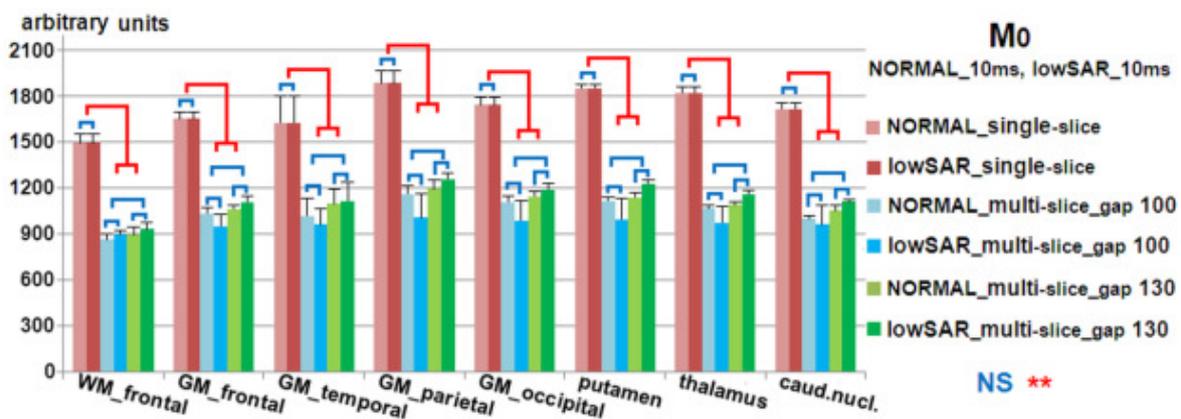


Fig.7. $M_0$ values from 8 regions in the healthy brain.
$M_0$ values were significantly higher (**, one-way ANOVA) in single-slice compared to the multi-slice measurements. The pulse duration "NORMAL" or "lowSAR" did not affect the calculation of $M_0$ (NS, unpaired t test) at the same echo spacing (10 ms) and bandwidth (275 Hz per pixel). It appeared that the size of the interslice gap did not affect calculating $M_0$ (NS, unpaired t test).

Table 1. $T_2$ relaxation times in the healthy brain.
For the $T_2$ mapping evaluation, 3 pixels were placed bilaterally in 8 regions in the brain. Data measurement was done by multi-echo CPMG sequence using multi-slice, echo spacing 7 ms, a bandwidth of 501 Hz per pixel and a 100 % interslice gap. We used standard pulse duration "NORMAL".

| region in the brain | $T_2$ [ms ± SD] |
|---|---|
| white matter-frontal | 84.2 ± 6.9 |
| gray matter-frontal lobe | 99.0 ± 17.3 |
| gray matter -temporal lobe | 99.8 ± 11.6 |
| gray matter -parietal lobe | 104.9 ± 14.6 |
| gray matter -occipital lobe | 106.3 ± 16.6 |
| putamen | 91.7 ± 9.9 |
| thalamus | 91.5 ± 10.0 |
| caudate nucleus | 91.8 ± 9.7 |

In the next step, we studied the $T_2$ relaxation times in 8 regions of the healthy brain (Table 1.). It appeared that the value of $T_2$ was not affected by inter-slice gaps (NS, unpaired t test) or by slice shifting. We observed that $T_2$ relaxation times in the single-slice sequence were not significantly different (one-way ANOVA) from $T_2$ values in multi-slice. Pulse duration "NORMAL" or "lowSAR" yielded similar values of $T_2$ (NS, unpaired Welch t), which was also true for the "NORMAL" pulses with shorter echo spacing and greater bandwidth (Fig.8.).

Furthermore, we found that the sequence with the "NORMAL" pulses had a lower SD of $T_2$ relaxation time than that of "lowSAR". Finally, we analyzed the echo spacing. We observed no significant difference (unpaired t test) in $T_2$ values when using the "NORMAL" pulse shapes with echo spacing 7 ms, 10 ms and 20 ms (Fig.9.). In addition, we found that the echo spacing of 20 ms achieved the greatest SD variance of $T_2$ relaxation times.
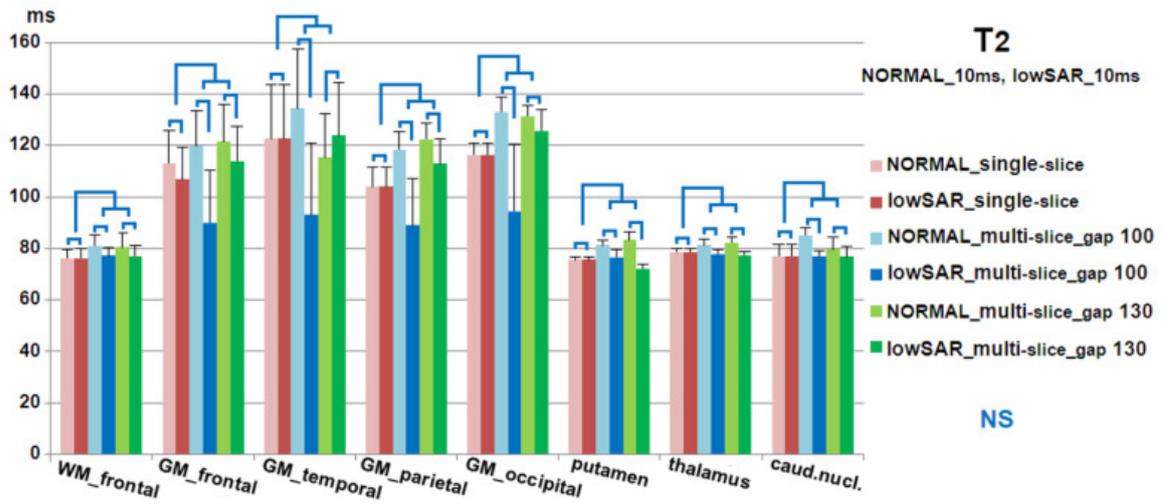
Fig.8. T$_2$ values in the healthy brain.
Pulse duration "NORMAL" or "lowSAR" did not affect T$_2$ values (NS, unpaired Welch t) at the same echo spacing (10 ms) or bandwidth (275 Hz per pixel). T$_2$ values were not significantly different (NS, one-way ANOVA) between single-slice and multi-slice measurements. The T$_2$ values were not affected by the size of inter-slice gap (NS, unpaired t test).
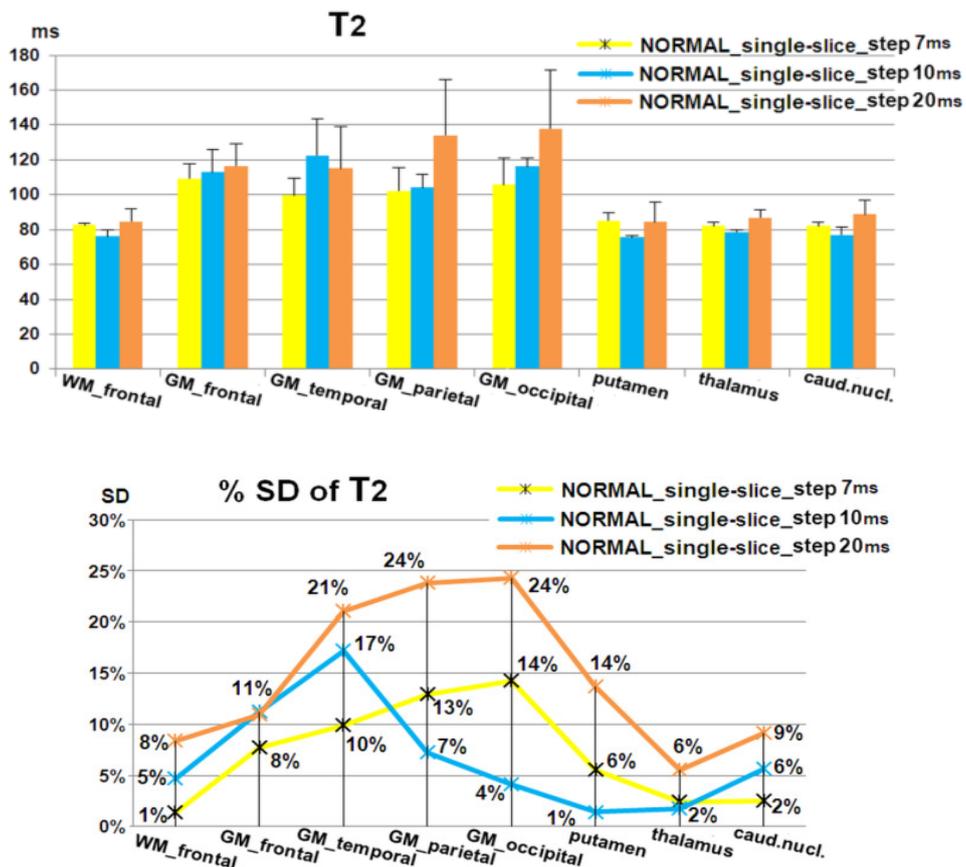




Fig.9. a, b. T$_2$ values and the graph of standard deviations (SD) of T$_2$ values in the healthy brain.
There was no significant difference (unpaired t test) in T$_2$ values between measurements with an echo spacing of 7 ms, 10 ms or 20 ms when using the "NORMAL" pulse duration. The measurement with echo spacing of 20 ms achieved greater SD variances of T$_2$ values in comparison to those that had shorter echo spacing.

## 4. DISCUSSION

The aim of our study was to test the influence of different adjustable protocol parameters of a standard multi-echo multi-slice CPMG sequence to the brain $T_2$ mapping on a 1.5 T whole-body MR scanner in the clinical radiological practice. For this purpose we have prepared and verified the experimental and data-processing part of the $T_2$ mapping. We constructed an MRI phantom with a wider range of $T_2$ relaxation times (28 ms < $T_2$ < 2200 ms), which covered the range of the healthy brain $T_2$ values (50 ms < $T_2$ < 110 ms) found in literature [3], [7], [24], [25], [33]. We decided to include longer $T_2$ values, because $T_2$s are generally prolonged in brain pathologies [12] - [24].

The decrease of $M_0$ due to incomplete $T_1$ relaxation in our measurements (TR=8860 ms) was found to be 1 % for the phantom with 4 % agarose concentration, 2 % for that with the 3 % concentration, 3 % for the 2 % concentration, and 4 % for the 1 % and 0 % agarose concentrations. This meant that 96 – 99 % of the magnetization was already recovered. Similar findings were found by measuring the $T_2$ relaxation time with TR 8860 ms in 8 regions of the healthy human brain (99 – 100 % of $M_0$ was relaxed).

The $M_0$ values characterize the signal to noise ratio (SNR) varying with the different measurement parameters ($T_1$ relaxation, number of slices, pulse duration, echo spacing, bandwidth, interslice gap and slice shifting). The lower SNR might negatively affect the accuracy of the $T_2$ maps. The fact that the noise level was the same in all images, allowed us to directly compare the calculated value of $M_0$ from measurements at various measurement conditions. Since there were no differences in $M_0$ values among various agarose concentrations measured with the same sequence, it confirmed that the incomplete $T_1$ recovery did not affect the accuracy of the calculation and estimation of the $T_2$.

It was confirmed that the magnetization $M_0$ was lower in the multi-slice compared to the single-slice sequence, which was probably related to the non-ideal excitation slice profiles. Although there was a lower SNR in the multi-slice experiments, reproducible data were obtained in the phantom as well as in the volunteer. This indicates that the multi-slice scan is suitable for $T_2$ mapping.

It can be expected that "lowSAR" pulses have a longer duration (and lower B1) to impose less SAR [38]. Longer pulses should provide a better defined profile of the slice and thus less contamination from the neighboring slices (and greater SNR). Indeed, the $M_0$ value measured in the "lowSAR" mode in the phantom was larger than that obtained with the "NORMAL" mode. However, the pulse duration did not significantly affect the $M_0$ values in the volunteer. This suggests that *in vivo* "NORMAL" pulse mode gives SNR comparable with that of the "lowSAR" mode in brain $T_2$ mapping.

In our last step, we studied the $T_2$ values using different protocol parameters (number of slices, pulse duration, echo spacing, bandwidth, interslice gap and slice shifting) in the phantom and in the volunteer. We obtained reproducible $T_2$ values in all multi-slice measurements. This was a favorable observation, since mapping of the whole organ is required in the clinical examinations.

Our custom-made software gave tools for providing the particular relaxation parameter maps and allowed the evaluation of various sizes of ROIs. We decided to choose smaller regions consisting of 6 pixels (3 voxels bilaterally), which were compact and without artifacts (arising from partial volume effect or point spread function), minimizing the influence of the signal from the edge of phantoms. The ROI positions and sizes were identical for all the scans with different measurement parameters, placed in the middle of phantoms. Furthermore, some studies emphasized the importance of choosing a small ROI size, due to the heterogeneity of the brain tissue [3], [41], [42]. In this article, we evaluated smaller ROIs positioned in 8 homogenous brain areas in order to cover different types of brain structures. Due to the choice of smaller ROIs and, therefore, a smaller analyzed data set throughout the experiment, we could only assume how the parameter values would change if there was a larger statistical data set. If the number of pixels increased, it would reduce the possibility of accidental errors. For clinical studies deeper analysis of various specific pathologies of the brain tissue would be useful to measure as big ROIs as allows the tissue heterogeneity and the nature of brain structures.

*In vitro* as well as *in vivo*, we found that the $T_2$ relaxation time was not affected by the pulse duration, even with the "NORMAL" pulse enabling shorter echo spacing and greater bandwidth. Therefore, due to the highest SNR, the "NORMAL" pulse duration with an echo spacing of 7 ms and bandwidth of 501 Hz per pixel is the most suitable setting for $T_2$ mapping in the brain.

We analyzed accuracy of $T_2$ mapping as a percentage of SD in $T_2$ values obtained in the phantom and in the volunteer. In phantoms, higher SD of $T_2$ meant less accuracy of the evaluation. In the brain *in vivo*, higher SD at higher $T_2$ did not represent only the accuracy, but also the heterogeneity of the brain tissue, particularly in the gray matter. Smaller echo spacing allowed the use of a larger number of data points with a shorter TE than expected in the $T_2$. It caused the SD reduction (therefore increased accuracy), particularly in shorter $T_2$s. In phantoms with longer $T_2$, their higher accuracy was only slightly reduced in measurements using smaller echo spacing. However, due to our clinical hardware limits, we were not able to go for shorter echo spacing, which might be even more appropriate.

Further, we confirmed, that neither slice shifting nor the size of inter-slice gap affected the $T_2$ mapping, in the phantom or in the volunteer. The minimum size of inter-slice gap was limited by the manufacturer to 100 %. It appeared that the extension to 130 % did not have any large influence on $M_0$ or $T_2$ values.

## 5. CONCLUSION

The CPMG multi-echo multi-slice sequence with the "NORMAL" pulse duration seems to be a suitable protocol for brain $T_2$ mapping. It was practical to measure 19 tissue slices for each of the 32 echo times with 7 ms echo spacing. For this sequence, a bandwidth of 501 Hz per pixel and a 100 % inter-slice gap were used. The *in vivo* measured and evaluated $T_2$ relaxation times (80 ms < $T_2$ < 106 ms) agreed

well with the values in the literature [3], [7], [24] – [26]. We believe that our results would be helpful for anyone mapping $T_2$ in the brain under clinical conditions, providing them measures of accuracy and optimum sequence parameters.

REFERENCES

[1] Parlato, M.B., Dzyubak, B., Helfenberger, J. Balge, N. (2009). *MRI phantom for fat quantification.* http://ebookbrowse.com/mri-phantom-for-fat-quantification-final-report-pdf-d96791611.

[2] Barker, P.B., Bizzi, A., De Stefano, N., Gullapalli, R., Lin, D.D.M. (2010). *Clinical MR Spectroscopy: Techniques and Applications* (1st ed.). Cambridge University Press.

[3] Georgiades, Ch.S., Itoh, R., Golay, X., van Zijl, P.C.M., Melhem, E.R. (2001). MR imaging of the human brain at 1.5 T: Regional variations in transverse relaxation rates in the cerebral cortex. *American Journal of Neuroradiology*, 22 (9), 1732-1737.

[4] Fanea, L., Sfrangeu, S.A. (2011). Relaxation times mapping using magnetic resonance imaging. *Romanian Reports in Physics*, 63 (2), 456-464.

[5] Kumar, R., Delshad, S., Woo, M.A., Macey, P.M., Harper, R.M. (2012). Age-related regional brain $T_2$-relaxation changes in healthy adults. *Journal of Magnetic Resonance Imaging*, 35 (2), 300-308.

[6] Deoni, S.C.L., Peters, T.M., Rutt, B.K. (2005). High-resolution $T_1$ and $T_2$ mapping of the brain in a clinically acceptable time with DESPOT1 and DESPOT2. *Magnetic Resonance in Medicine*, 53 (1), 237-241.

[7] Deoni, S.C.L., Josseau, M.J., Rutt, B.K., Peters, T.M. (2005). Visualization of thalamic nuclei on high resolution, multi-averaged $T_1$ and $T_2$ maps acquired at 1.5T. *Human Brain Mapping*, 25 (3), 353-359.

[8] McRobbie, D.W., Moore, E.A., Graves, M.J., Prince, M.R. (2007). *MRI from Picture to Proton* (2nd ed.). Cambridge University Press.

[9] Bartzokis, G., Sultzer, D., Cummings, J. et al. (2000). In vivo evaluation of brain iron in Alzheimer disease using magnetic resonance imaging. *Archives of General Psychiatry*, 57 (1), 47-53.

[10] Pell, G.S., Briellmann, R.S., Waites, A.B., Abbott, D.F., Lewis, D.P., Jackson, G.D. (2006). Optimized clinical $T_2$ relaxometry with a standard CPMG sequence. *Journal of Magnetic Resonance Imaging*, 23 (2), 248-252.

[11] McKenzie, C.A., Chen, Z., Drost, D.J., Prato, F.S. (1999). Fast acquisition of quantitative $T_2$ maps. *Magnetic Resonance in Medicine*, 41 (1), 208-212.

[12] Hendry, J., DeVito, T., Gelman, N. et al. (2006). White matter abnormalities in autism detected through transverse relaxation time imaging. *NeuroImage*, 29 (4), 1049-1057.

[13] Supprian, T., Hofmann, E., Warmuth-Metz, M., Franzek, E., Becker, T. (1997). MRI $T_2$ relaxation times of brain regions in schizophrenic patients and control subjects. *Psychiatry Research: Neuroimaging*, 75 (3), 173-182.

[14] Ongur, D., Prescot, A.P., Jensen, J.E. et al. (2010). $T_2$ relaxation time abnormalities in bipolar disorder and schizophrenia. *Magnetic Resonance in Medicine*, 63 (1), 1-8.

[15] Woermann, F., Barker, G., Birnie, K., Meencke, H., Duncan, J. (1998). Regional changes in hippocampal $T_2$ relaxation and volume: A quantitative magnetic resonance imaging study of hippocampal sclerosis. *Journal of Neurology, Neurosurgery and Psychiatry*, 65 (5), 656-664.

[16] Vymazal, J., Righini, A., Brooks, R.A. et al. (1999). $T_1$ and $T_2$ in the brain of healthy subjects, patients with Parkinson disease, and patients with multiple system atrophy: Relation to iron content. *Radiology,* 211 (2), 489-495.

[17] Taylor, I., Butzkueven, H., Litewka, L. et al. (2004). Serial MRI in multiple sclerosis: A prospective pilot study of lesion load, whole brain volume and thalamic atrophy. *Journal of Clinical Neuroscience*, 11 (2), 153-158.

[18] Stevenson, V.L., Parker, G.J., Barker, G.J. et al. (2000). Variations in $T_1$ and $T_2$ relaxation times of normal appearing white mater and lesions in multiple sclerosis. *Journal of the Neurological Science*, 178 (2), 81-87.

[19] Oh, J., Cha, S., Aiken, A.H. et al. (2005). Quantitative apparent diffusion coefficients and $T_2$ relaxation times in characterizing contrast enhancing brain tumors and regions of peritumoral edema. *Journal of Magnetic Resonance Imaging*, 21 (6), 701-708.

[20] Yamada, S., Kubota, R., Yamada, K., Ono, S., Hishinuma, T., Matsuzawa, T., Fujiwara, S. (1990). $T_1$ and $T_2$ relaxation times on gadolinium – diethylenetriaminepentaacetic acid enhanced magnetic resonance images of brain tumors. *Tohoku Journal of Experimental Medicine*, 160 (2), 145-148.

[21] Radiology. (2012). Book Reviews: Quantitative MRI in Cancer. *Radiology*, 264 (1), 38-39.

[22] Vymazal, J., Babis, M., Brooks, R.A., Filip, K., Dezortova, M., Hrncarkova, H., Hajek, M. (1996). $T_1$ and $T_2$ alterations in the brains of patients with hepatic cirrhosis. *American Journal of Neuroradiology*, 17 (2), 333-336.

[23] Chang, K.J., Jara, H. (2004). Applications of quantitative $T_1$, $T_2$, and proton density to diagnosis. *Applied Radiology*, 34 (1), 34-42.

[24] Whittall, K.P., MacKay A.L., Graeb, D.A., Nugent, R.A., Li, D.K.B., Paty, D.W. (1997). In vivo measurement of $T_2$ distributions and water contents in normal human brain. *Magnetic Resonance in Medicine*, 37 (1), 34-43.

[25] Zhou, J., Golay, X., van Zilj, P.C. et al. (2001). Inverse $T_2$ contrast at 1.5 Tesla between gray matter and white matter in the occipital lobe of normal adult human brain. *Magnetic Resonance in Medicine,* 46 (2), 401-406.

[26] Deoni, S.C., Rutt, B.K., Peters, T.M. (2003). Rapid combined $T_1$ and $T_2$ mapping using gradient recalled acquisition in the steady state. *Magnetic Resonance in Medicine*, 49 (3), 515-526.

[27] Herynek, V., Wagnerova, D., Hejlova, I., Dezortova, M., Hajek, M. (2012). Changes in the brain during long-term follow-up after liver transplantation. *Journal of Magnetic Resonance Imaging*, 35 (6), 1332-1337.

[28] Whitaker, Ch.D.S. (2004). *Evaluation of Hahn, CPMG, and combined spin echo analysis at 8 Tesla MRI*. Doctoral dissertation, Ohio State University.

[29] Deoni, S.C., Rutt, B.K., Arun, T., Pierpaoli, C., Jones, D.K. (2008). Gleaning multicomponent $T_1$ and $T_2$ information from steady-state imaging data. *Magnetic Resonance in Medicine*, 60 (6), 1372-1387.

[30] Madler, B., MacKay, A.L. (2006). In vivo 3D multi-component $T_2$ relaxation measurements for quantitative myelin imaging at 3T. In *Proceedings of the 14th Annual Meeting of ISMRM*. Seattle, WA, USA.

[31] Stefanovic, B., Sled, J.G., Pike, G.B. (2003). Quantitative $T_2$ in the occipital lobe: The role of the CPMG refocusing rate. *Journal of Magnetic Resonance Imaging*, 18 (3), 302-309.

[43]

[32] Petrov, O.V., Balcom, B.J. (2011). Two-dimensional $T_2$ distribution mapping in porous solids with phase encode MRI. *Journal of Magnetic Resonance*, 212 (1), 102-108.

[33] Yoshimura, K., Kato, H., Kuroda, M. et al. (2003). Development of a tissue-equivalent MRI phantom using carrageenan gel. *Magnetic Resonance in Medicine*, 50 (5), 1011-1017.

[34] Hungr, N., Long, J.A., Beix, V., Torccaz, J. (2012). Supplemental material 2 - Phantom storage properties. *Medical Physics*, 39 (4), 2031-2041.

[35] Price, R.R., Axel, R. Morgan, T. et al. (1990). Quality assurance methods and phantoms for magnetic resonance imaging. *Medical Physics,* 17 (2), 287-295.

[36] Bushong, S.C. (2003). *Magnetic Resonance Imaging* (3rd ed.). Mosby Publisher.

[37] Runge, V.M., Nitz, W,R., Schmeets, S.H., Schoenberg, S.O. (2011). *Clinical 3T Magnetic Resonance*. Thieme Medical Publisher.

[38] Graessner, J. (2013). Bandwidth in MRI? *MAGNETOM Flash,* 2, 3-8.

[39] Hashemi, R.H., Bradley, W.G. Jr., Lisanti, Ch.J. (2010). *MRI: The Basics* (3rd ed.). Lippincott Williams & Wilkins, Philadelphia.

[40] De Graaf, R.A. (2007). *In vivo NMR Spectroscopy: Principles and Techniques* (2nd ed.). Wiley.

[41] Kumar, R., Delshad, S., Macey, P.M., Woo, M.A., Harper, R.M. (2011). Development of $T_2$-relaxation values in regional brain sites during adolescence. *Magnetic Resonance Imaging*, 29 (2), 185-193.

[42] Jokivarsi, K.T., Hiltunen, Y., Grohn, H. et al. (2010). Estimation of the onset time of cerebral ischemia using $T_1$ and $T_2$ MRI in rats. *Stroke,* 41 (10), 2335-2340.